

# Resonant Energy Transport in Dye-Filled Monolithic Crystals of Zeolite L: Modeling of Inhomogeneity

Lucas Viani,<sup>\*,†</sup> Andrea Minoia,<sup>‡</sup> Jérôme Cornil,<sup>‡</sup> David Beljonne,<sup>‡</sup> Hans-Joachim Egelhaaf,<sup>§,ID</sup> and Johannes Gierschner<sup>\*,||,ID</sup>

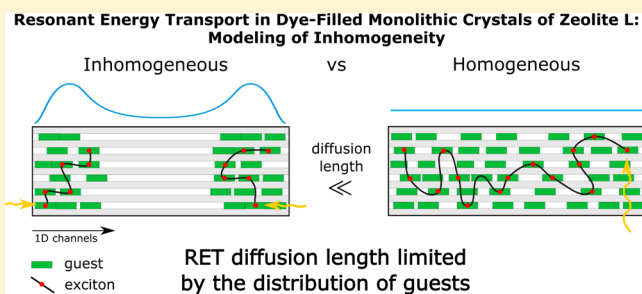
<sup>†</sup>Institute for Fluid Dynamics, Nanoscience and Industrial Mathematics, Universidad Carlos III De Madrid, Av. De La Universidad 30, Leganes E-28911, Spain

<sup>‡</sup>Laboratory for Chemistry of Novel Materials, University of Mons, Place du Parc 20, B-7000 Mons, Belgium

<sup>§</sup>ZAE Bayern-Solar Factory of the Future, Energy Campus Nürnberg, Fürtherstr. 250, 90429 Nürnberg, Germany

<sup>||</sup>Faculty of Science Module C-IX, Madrid Institute of Advanced Studies (IMDEA Nanoscience), C/ Faraday 9, Ciudad Universitaria de Cantoblanco, E-28049 Madrid, Spain

**ABSTRACT:** Resonant energy transfer (RET) is a key mechanism in organic optoelectronic devices, and its efficiency depends critically on the intermolecular arrangement of the active compounds. Supramolecular organization promoted by nanostructured supramolecular host–guest compounds (HGCs) is an elegant way of controlling the packing of the molecules inserted in optically inert organic or inorganic host materials. Under ideal conditions (i.e., dye properties and homogeneous distribution) very high exciton diffusion rates are expected in zeolite L HGCs, being of high relevance for practical applications. From experiment, however, there is clear evidence for inhomogeneity dependent on the type of chromophore, the preparation procedure, and the size of host crystals, but the reason for inhomogeneity and the consequences on exciton diffusion are under debate. In this work we elucidate these issues making use of computational tools (dynamic Monte Carlo and molecular dynamics) to elucidate the RET dynamics in the inorganic zeolite L taking into account the inhomogeneity of the dye distribution along the 1D channels.



## 1. INTRODUCTION

Resonant energy transfer (RET) is a key mechanism in organic optoelectronic devices such as organic photovoltaic cells (OPVs) and light-emitting diodes (OLEDs). However, the RET efficiency critically depends on the intermolecular arrangement of the conjugated organic compounds and might fluctuate over a large range. An elegant route toward materials with high RET efficiencies relies on nanostructured supramolecular host–guest compounds (HGCs).<sup>1,2</sup> Herein, photo- and electroresponsive molecules are spatially organized inside nano- and subnanoscale cavities of channel-forming optically inert organic<sup>3–8</sup> or inorganic<sup>9–11</sup> host materials. The channels promote a better chemical stability and reduction of positional and energetic disorder among guests by constraining their motion to virtually one dimension.<sup>3,7,12–16</sup> The inclusion of a variety of well-defined oligomers with tailor-made properties,<sup>17,18</sup> and in high concentrations,<sup>3</sup> allows for brightly emissive color-tuned systems,<sup>5,9,19–24</sup> while avoiding emission quenching by H-aggregation.<sup>25</sup> The large variety of organic<sup>18</sup> and inorganic host materials<sup>9,22,26</sup> promotes HGCs as a flexible tool in designing novel supramolecular architectures, where the crystals can be macroscopically oriented on surfaces in a strict unidirectional way, as demonstrated for zeolite L.<sup>2,27,28</sup> A key feature for the application of HGCs is the possibility to connect

the guest molecules to the outside world via the so-called molecular stopcocks<sup>7,29</sup> allowing for the extraction or injection of charges or excitons.<sup>29–32</sup> Such stopcocks were demonstrated both for inorganic<sup>26,33,34</sup> and organic hosts.<sup>35</sup> Because of the large variety of available host materials, it is possible to select the best combination of crystal size and aspect ratio as well as size and nature of the cavities for a given application.

For subnanometer channels (with diameters of 5–10 Å), a special attention was paid to organic perhydrotriphenylene (PHTP)<sup>19</sup> and to inorganic zeolite L as hosts.<sup>9</sup> Both systems share a hexagonal nanochannel arrangement with rather similar interchannel separations of about 14 and 18 Å,<sup>1,9,19</sup> respectively. However, detailed spectroscopic studies reveal very different host–guest interactions. The neutral guest chromophores in PHTP are embedded in a tight but soft, unspecific, and homogeneous van der Waals (vdW) environment allowing for some intramolecular vibrational and rotational degrees of freedom.<sup>7</sup> The close vdW contact of the collinear arranged guests gives rise to collective guest dynamics.<sup>36</sup> On the other hand, the neutral or cationic guests

**Received:** October 4, 2016

**Revised:** November 6, 2016

**Published:** November 7, 2016

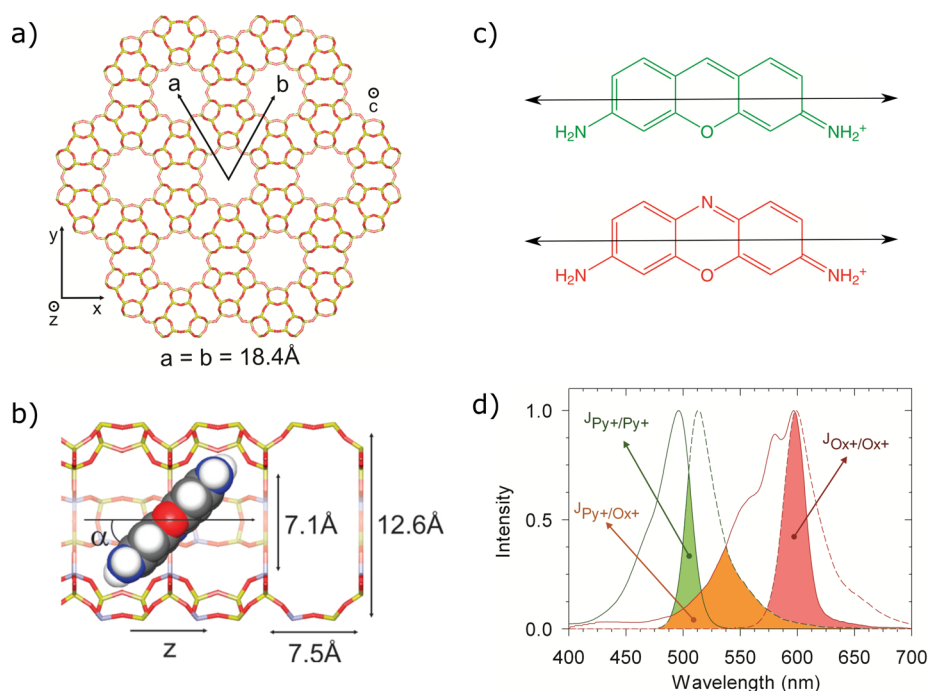


**Figure 1.** (a) Top view of a zeolite L crystal in the direction of the channel axis  $c$ . (b) Small and large diameter values and length of the cavities along the channel. (c)  $P_y^+$  and  $O_x^+$  structures; the TDMs of the  $S_0 \rightarrow S_1$  transition are indicated. (d) Emission and absorption spectra of  $P_y^+$  and  $O_x^+$  in zeolite L obtained from ref 45; spectral overlaps are highlighted.

in zeolite L experience in some cases specific interactions with the charges inside the host cavities,<sup>24,31,37</sup> while in other cases no or very little changes in the absorption and fluorescence spectra of the guests have been observed.<sup>16,38</sup> This seems to characteristically influence the dye distribution inside the channels, and the luminescent behavior of the embedded dyes,<sup>39</sup> and is expected to have a particular impact on the RET dynamics. However, up to now, the theoretical description of RET inside zeolite L was limited to the classical Förster model, where interactions were described through homogeneously or quasi-homogeneously distributed point dipoles.<sup>11,40</sup> In the framework of this model, very efficient RET dynamics were predicted for pyronine (py-loaded zeolite L with diffusion length in the micrometer range),<sup>40</sup> a result highly relevant for the application of such systems in optoelectronic devices. This is remarkably higher than that of distyrylbenzene (DSB) in PHTP (75 nm), mainly due the better photophysics characteristics (spectral overlap, exciton coupling, excited state lifetime) of pyronine compared to DSB.

On the other hand, detailed joint computational and experimental studies on RET in PHTP HGCs clearly showed that a correct description has to go beyond the point-dipole approximation (PDA) and use a more precise quantum-chemically (QC) enhanced Förster model embedded in a macroscopic Monte Carlo (MC) scheme.<sup>4,41</sup> The success of this work encouraged us to apply the same scheme to zeolite L HGCs in order to fully elucidate the real RET dynamics in zeolite L at the nanoscale, with a main focus on the role of inhomogeneity in the dye distribution within the nanostructures.<sup>42</sup> Interestingly, our molecular dynamics simulations provide evidence for a cooperative blocking mechanism inside the channels.

## 2. SYSTEM DESCRIPTION

Zeolite L has been extensively studied in the past for light harvesting<sup>9,43,44</sup> and conversion,<sup>45,46</sup> white light-emitting devices,<sup>47</sup> and medical applications.<sup>48,49</sup> It features hexagonally arranged 1D nanochannels with an interchannel distance of 18.4 Å. Each channel consists of connected cavities with a length of 7.5 Å, a free vdW diameter at the entrance of 7.1 Å, and at the center of 12.6 Å<sup>9</sup> (see Figure 1a,b). The zeolite L channels are filled by inserting cationic dyes through ion exchange,<sup>9</sup> where the occupation probability of the dyes in the channel is dependent on the dye concentration in the solution and the diffusion time.<sup>9</sup> Multiple guest inclusions can be achieved by simultaneous insertion, e.g. with a 1:1 ratio, as used in the present work. In particular, pyronine and oxonine guest molecules (see Figure 1c) acting as donor (D) and acceptor (A), respectively, are ideal for this purpose, since their similar chemical structure leads to a comparable diffusion behavior. Their high photoluminescence (PL) quantum yields make  $P_y^+$  and  $O_x^+$  interesting for applications in self-assembling micro-objects.<sup>29,47,50–52</sup> The large spectral overlap of the pyronine PL spectrum with the absorption of pyronine ( $P_y^+/P_y^+$ ) and oxonine ( $P_y^+/O_x^+$ ) as well as the long PL lifetime of  $P_y^+$  (3.2 ns) and large  $P_y^+/P_y^+$  exciton couplings (*vide infra*) promote high RET efficiencies for both D–D and D–A transfer steps (Figure 1d).

The cavities in the channels allow for molecular wobbling motions<sup>36,53–56</sup> characterized by a cone angle,  $\alpha$ , between the channel axis and the long molecular axis, as depicted in Figure 1b. As we will see later, this type of motion will affect RET dynamics in different ways: (i) by changing the relative orientation of the transition dipole moment (TDM) vectors of the molecules, which may influence the magnitude of the transfer rate and the directionality of the diffusion; (ii) by allowing formation of molecular aggregates;<sup>57,58</sup> (iii) by promoting the blockage of channels leading to an inhomoge-

neous distribution of dyes along the channels.<sup>33,43,51</sup> Experimentally, the distribution of  $\alpha$  values has been investigated by means of PL anisotropy imaging<sup>53</sup> and by polarized two-photon (TP) PL microscopy.<sup>54</sup> Both techniques are based on the measurement of the orientation of the TDM of the lowest electronic excited state,  $S_0 \rightarrow S_1$ , which in  $P_y^+$  and  $O_x^+$  coincide with the long molecular axis (see Figure 1c). Thus, changes in the TDM orientation are directly linked to changes in the molecular orientation. In the case of  $O_x^+$ , ref 53 reports a cone angle of  $72^\circ$  while the detailed TP-PL analysis in ref 54 gives  $77^\circ$  with a distribution of  $24^\circ$ . Similar values are expected for  $P_y^+$  due to the similar geometries. These values differ from those based on geometric restriction,  $\sim 30^\circ$  and  $\sim 65^\circ$ , which may be linked to the presence of charges inside the zeolite L crystal that induce distortions of the TDMs, as suggested in refs 53, 55, and 39.

Theoretical studies on RET dynamics in zeolite L have been limited to calculations based on the Förster equation for D–D and D–A transfer steps in its original formulation, i.e., using the point dipole approximation (PDA), by solving the master equations (Markov chain),<sup>40</sup> and by performing Monte Carlo (MC) simulations.<sup>11</sup> In both cases, the distribution of guests and voids throughout the channels was assumed to be homogeneous<sup>40</sup> (or quasi-homogeneous<sup>11</sup>). Within such a framework, an energy diffusion constant of  $7.0 \times 10^{-2} \text{ cm}^2 \text{ s}^{-1}$  was predicted for a completely  $P_y^+$ -filled crystal, which corresponds to a diffusion length of about  $2 \mu\text{m}$ .<sup>40</sup>

However, even for weakly coupled systems, the PDA might be inappropriate for describing the RET dynamics. In fact,<sup>9,41</sup> investigations on 3D RET processes in PHTP-based HGCs for varying D–D distances<sup>19</sup> have revealed that even for such weakly coupled systems, a quantitative theoretical description has to go beyond the PDA to correctly reproduce the RET dynamics. This is done here by replacing the PDA with a more precise quantum-chemical approach based on atomic transition densities (see section 2), within a diffusion-enhanced Förster model (i.e., including donor–donor (DD) steps) embedded in a macroscopic Monte Carlo (MC) scheme with no adjustable parameters. For PHTP-based HGCs, this method has proven to be able to reproduce accurately the measured steady-state RET efficiency as a function of the molar doping ratio as well as the time-resolved PL time traces of donor and acceptor dyes. Furthermore, it allowed to fully quantify the RET dynamics in the PHTP HGCs, providing exciton diffusion lengths on the order of  $75 \text{ nm}$  for distyrylbenzene as guest species.<sup>41</sup> In the following, we will thus apply this scheme to the RET dynamics in dye-loaded zeolite L; for computational details see section 2.

### 3. COMPUTATIONAL DETAILS

**Monte Carlo Scheme.** In the MC approach, pyronine ( $P_y^+$ ) and oxonine ( $O_x^+$ ) molecules (see Figure 1) are placed into a  $99 \times 99$  grid of hexagonally organized channels with interchannel separations of  $18.4 \text{ \AA}$ .<sup>9</sup> To generate the morphology in a realistic way, nonuniform intermolecular distances, molecular voids, random positional disorder along the channels, inhomogeneous distribution of dyes, and possible wobbling motions are considered. The molecular orientation, and hence the orientation of the transition dipole moment (TDM), followed a random angular distribution at the surface of a cone with a fixed angle  $\alpha$  against the channel axis (see Figure 1).

Every MC simulation is based on a morphology individually designed to mimic the measured length, loading, and distribution of molecules along the channels for a specific

zeolite L crystal, as obtained from confocal microscopy (CM) intensity graphs. The number of molecules in the host is defined by the respective molecular loadings,  $p$ , defined as the ratio between the number of guest molecules and the number of sites available in the crystal (in this case, the number of available sites equals the number of zeolite L unit cells/2).<sup>9</sup> The molecules are randomly distributed along the channels according to a predefined molecular distribution probability. In this procedure, the smallest intermolecular distance allowed inside a channel is set to be equal to their vdW distance. Molecular rotations are randomly applied to every molecule independently, respecting the constraints of the environment. Like this, systems featuring a crystal loading lower than 1 will naturally present voids along the channels. For each hopping event, all the transfer rates to donor,  $k_{DD}$ , and acceptor sites,  $k_{DA}$ , are calculated for molecules inside a predefined cutoff region defined as a cylinder of  $80 \text{ nm}$  radius and  $200 \text{ nm}$  length with the excited molecule placed in its center. The size of the cutoff lattice was chosen so that RET to sites outside of the cutoff lattice is negligible. Since the simulations were performed over crystals with realistic sizes and molecular loadings, no periodic boundary condition was applied. The MC trajectories were calculated following the same scheme as used in refs 4 and 41.

**RET Rates.** The description of the energy transfer rates is derived via Fermi's golden rule as

$$k_{\text{ET}} = \frac{2\pi}{\hbar} |V_{\text{DX}}|^2 s^2 J_{\text{DX}} \quad (1)$$

where  $V_{\text{DX}}$  is the excitonic coupling between a pair of molecules, with X being donor (D) or acceptor (A),  $s$  the screening factor, and  $J_{\text{DX}}$  the spectral overlap between the emission spectrum of D and the absorption spectrum of X, both area-normalized on the energy scale. As shown earlier,<sup>4</sup> the classical Förster point-dipole approach (PDA) can be only used to describe the excitonic couplings in HGCs for low dye concentrations, i.e., large intermolecular separations. Otherwise, the PDA underestimates intrachannel and overestimates interchannel transfer rates, respectively, affecting the directionality of the diffusion process. Since in this work we are interested on different loading ratios, and the directionality is a key property in understanding exciton migration, we have adopted the more general distributed monopole approach to calculate all excitonic couplings, which are estimated as

$$V_{\text{DX}} = \frac{1}{4\pi\epsilon_0} \sum_{i,j} \frac{q_{\text{D}}^i q_{\text{X}}^j}{R_{\text{DX}}^{ij}} \quad (2)$$

where  $q_{\text{D}}^i$  and  $q_{\text{X}}^j$  are the atomic transition densities (ATD) over atoms belonging to molecules D and X, respectively, and  $R_{\text{DX}}^{ij}$  is the distance between them. The screening factor  $s$  was considered to be  $1/n^2$ , i.e., like in the PDA. ATD values were determined from ZINDO/S calculations (Zerner's spectroscopic parametrization for the semiempirical Hartree–Fock intermediate neglect of differential overlap method)<sup>59</sup> on the basis of geometries optimized at the semiempirical Hartree–Fock AM1 (Austin Model 1) level,<sup>60</sup> imposing planar conformations for the conjugated backbone.

**MD Simulations.** Molecular dynamics simulations have been used to investigate the diffusion of the oxonine molecule,  $O_x^+$  along the channels. All simulations have been carried out using the molecular modeling package Materials Studio 5 with its implemented version of the CVFF force field, which is able

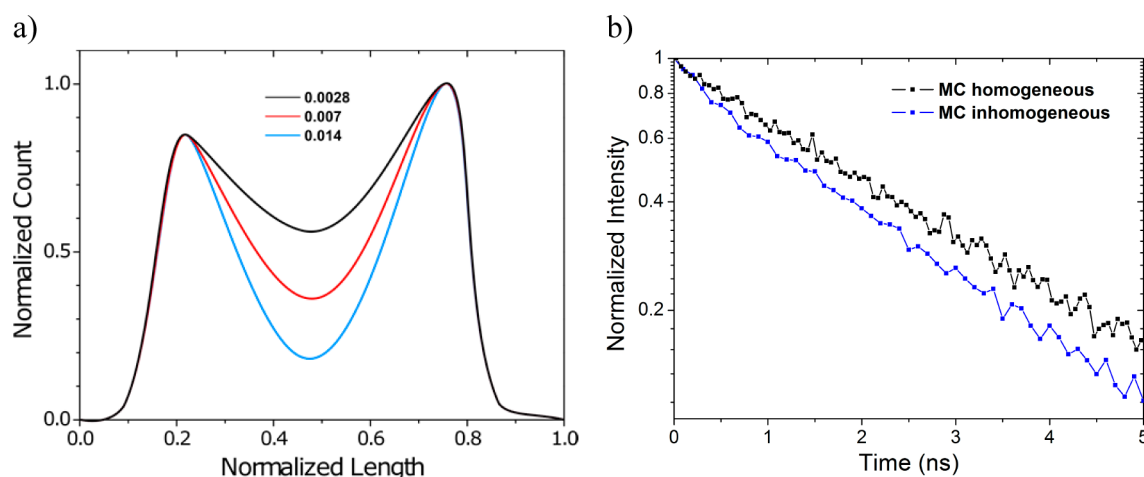


**Figure 2.** (a) Molecular distribution obtained from CM images in ref 33 (black lines) and estimated from CM images in ref 57 for lower concentrations. (b) Simulated time traces of the donor PL at a loading of  $p = 0.014$  over a homogeneous (black) and inhomogeneous (blue) distribution of guests.

to properly describe the interactions in hybrid organic–inorganic systems. The host system is a single zeolite L channel, made of six cavities in the unit cell which is replicated by using 3D periodic boundary conditions. According to XRD diffraction data,<sup>61</sup> in the aluminosilicate version of the zeolite L, nine silicon atoms are randomly replaced by aluminum atoms. Since the O–Al–O bridges have a negative net charge of  $-1$ , the framework of the aluminosilicate zeolite L is negatively charged, and therefore, cations ( $K^+$ ) are introduced to neutralize the total charge. In our model, we have modified the all silica LTL structure by placing nine aluminum atoms and nine cations per cavity. Aluminum atoms have been randomly placed with the only constraint of avoiding the formation of Al–O–Al bridges, which are chemically unstable. Simulations are conducted in the NVT ensemble. The channel has been treated as a rigid body fixed in space, since no vibrational cooperative motions are expected due to the reduced width of the dyes considered.<sup>62</sup>

#### 4. RESULTS AND DISCUSSION

The shape of the dye distribution in zeolite L channels has proven to be an important property in the description of the RET dynamics. The guest distribution is affected by different factors, for instance, the structure of the dyes, the preparation conditions, and the size of the crystals. It can be estimated experimentally by performing confocal microscopy (CM) measurements on single crystals. In the specific case of  $P_y^+$ , the CM measurements published in refs 33 and 57 can be considered as an example of a typical room temperature frozen situations, showing high dye concentrations relatively close to the channel entrances, while it is much lower in the center of the crystal (*vide infra*). It also shows that the diffusion of the dyes through the channels is slowed down or even blocked as the concentration of guest increases from 0.6 to 20%. It should be stressed that the intensity distribution obtained from CM measurements should represent the dye distribution if quenching by aggregation is small. The guest distributions used in the MC simulations are based on the CM data in refs 33 and 57 providing a better way to reproduce the distribution of the dyes for a given concentration (see Figure 2a). The edges of the crystals were set in a similar manner as that shown in ref 33.

RET dynamics were investigated considering crystals with a length of 3–4.5  $\mu\text{m}$  and a diameter of  $\sim 1 \mu\text{m}$  with four different loadings  $p_1 = 0.014$ ,  $p_2 = 0.007$ , and  $p_3 = 0.0028$  of  $P_y^+$  and  $O_x^+$  molecules acting as donor and acceptor, respectively, in a 1:1 ratio. In order to model the RET dynamics, we have applied the MC scheme developed in refs 4 and 41 to the zeolite L crystal. The RET rates were obtained on the basis of a generalized (quantum-chemical-based) Förster model;<sup>4</sup> for details see section 2. The molecular orientation was set to follow a random angular distribution along the surface of a cone with a fixed angle  $\alpha = 77^\circ$  (see Figure 1b). The experimental parameters used in the simulations include the spectral overlaps (see Figure 1d;  $J_{P_y^+/P_y^+} = 1.72 \times 10^{-4} \text{ cm}$ ,  $J_{P_y^+/O_x^+} = 1.38 \times 10^{-4} \text{ cm}$ ) and PL lifetimes ( $\tau_{P_y^+,0} = 3.0 \text{ ns}$ ,  $\tau_{O_x^+,0} = 3.2 \text{ ns}$ );<sup>45</sup> no adjustable parameters were used.

In a first step, we investigated the impact on the time traces of considering either a homogeneous or an inhomogeneous dye distribution within the channels of zeolite L. As shown in Figure 2, the donor decay significantly slows down (by a factor  $\sim 3$ ) when going from an inhomogeneous to a homogeneous distribution. Thus, the assumption of a homogeneous distribution of dyes within the channels used in refs 11 and 40 has to be treated carefully, and the determination of the distribution of guests along the channels must first be assessed for a correct interpretation of the experimental data.

At first sight, the population along the channels in ref 57 is rather counterintuitive since one might expect crystals with higher molecular concentrations to feature a higher population of guests toward the center of the channels in order to better accommodate the larger number of guest molecules. It suggests a transient blocking regime in which the first molecule blocks the channel, with its degrees of freedom (rotational and translational) hindered by the adjacent molecules in the channel. The probability of unblocking the channel is expected to drastically decrease with the increase in the loading levels, delaying the diffusion process. This scenario is depicted in Figure 3.

In order to gain a better insight into the dye diffusion process, MD simulations have been performed for one  $O_x^+$  molecule included in an empty zeolite L channel at high temperature ( $T = 500 \text{ K}$ ) in order to promote the diffusion process. The simulations were performed in dry conditions;

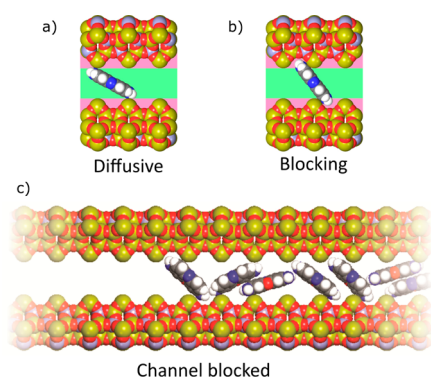


**Figure 3.** Cartoon illustrating the possible arrangements of guests leading to the diffusive (a) and the transient blocking regime (b). (c) Illustration of the cooperative blocking mechanism in a channel, which may be responsible for stopping the diffusion process inside the channel.

thus, no solvent–guest interactions are present.<sup>55</sup> During the 10 ns of the simulations the molecule was able to change its orientation with respect to the axis of the channel, but not to diffuse translationally, despite the high temperature used. To shed light on this behavior, we calculated the energy profile associated with the diffusion process. To do so, the molecule is initially positioned in the middle of the first cavity with its long axis aligned with the channel axis. The molecule is then moved along the channel by steps of 2 Å for a total displacement of 20 Å, scanning ten different locations along three cavities of the channel (Figure 5a). For each position, we have (i) calculated the total energy of the system and (ii) performed a geometry optimization by relaxing the system, i.e., the geometry and the position of the molecule inside the channel. Figure 4b shows the corresponding lowest energy conformations. It is important to note here that regardless of the initial position, the optimization brings the molecule close to the channel wall in between two adjacent cavities, as depicted by the geometry shown in Figure 4b.

The energetic profiles for the initial (labeled as SP) and optimized (labeled as Opt) geometries are reported in Figure 4c. The plot for SP shows that in order to diffuse, the molecule has to cross large energetic barriers, which may explain why the

inclusion is slow and the zeolite channels cannot be filled up completely. The energy profile obtained for the optimized geometries shows that the energy varies along the channel, despite the fact that the molecule adopts similar final conformations. This is due to (i) the random distribution of aluminum sites in the channel, which breaks the translational symmetry of the channel, and (ii) the strong interactions between the oxygen in the molecule and the negatively charged O–Al–O bridges in the zeolite framework. The aluminum sites act as sort of traps for the molecule, thus being responsible for the slow molecular diffusion in the channel.

The influence of the concentration of dyes in the exciton dynamics was studied by considering three systems s1, s2, and s3, with loading of 0.014, 0.007, and 0.000 28, respectively. The concentrations and the respective distributions (see Figure 2) were chosen in order to match the systems in ref 57. Based on the shape of the distributions, it is evident that by lowering the concentration, the molecules diffuse to the inside of the channels creating a more homogeneous distribution. It has a direct impact on the exciton lifetime, since the more diffuse the molecules are the lower is the number of excitations quenched via DA transfer due to the larger intrachannel intermolecular separations<sup>45</sup> (see illustration in Figure 6). This is confirmed by the predicted lifetimes amounting for 1.7, 2.4, and 2.7 ns, as extracted from the donor time traces (see Figure 5) for the systems s1, s2, and s3, respectively.

Another property affected by the concentration of dyes is the directionality of the exciton migration, since for the highly loaded system; the transport takes place mainly along the channels, while for lower concentrations, the transport is balanced between inter- and intrachannel steps. An average reduction of 60% in the interchannel transfer steps are observed when going from the highest to the lowest loaded system, while the number of intrachannel transfers remains at constant values. It directly translates into a reduction in the exciton diffusion length, with a gradual transition from 3.8 to 1.5 nm, as the concentration increases. It is important to note that these diffusion lengths are much shorter than the 800 nm diffusion obtained for a fully P<sub>y</sub><sup>+</sup>-loaded homogeneously distributed system. Such highly loaded systems are however challenging to be constructed with rod-shaped molecules featuring dimensions

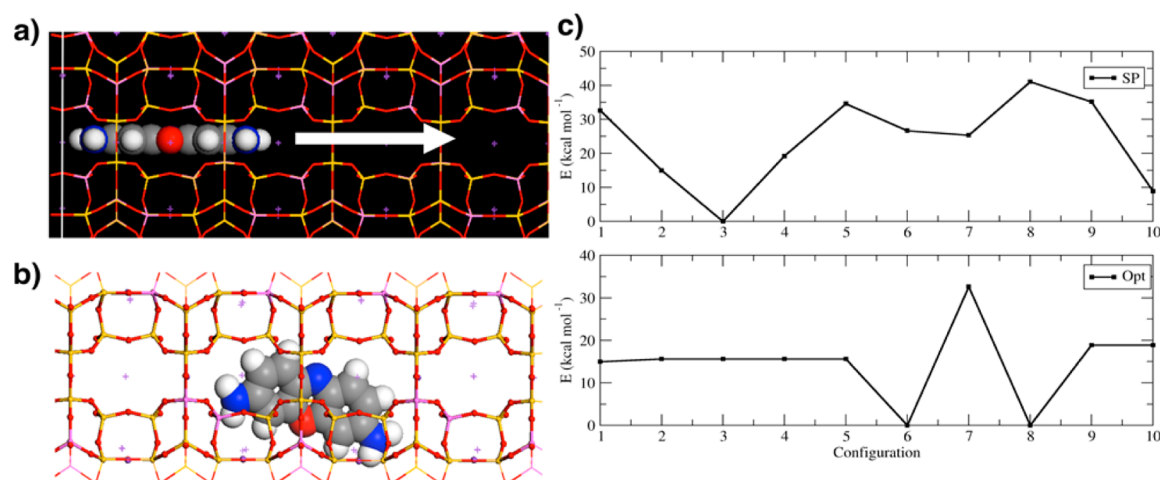


**Figure 4.** (a) Schematic illustration of the process used to calculate the diffusion energy profile. (b) Most stable optimized geometry obtained from the calculations. (c, top panel) Diffusion energy profile obtained when translating rigidly the molecule. (c, bottom panel) Diffusion energy profile obtained by optimizing the geometry at each position.

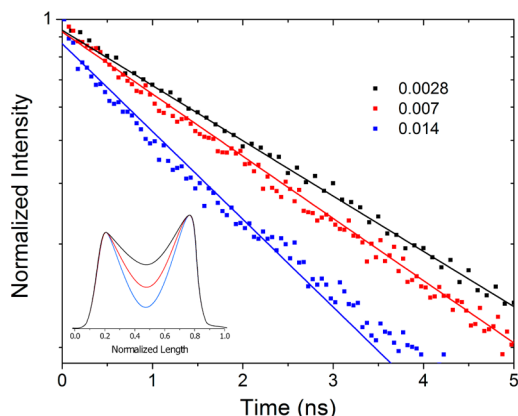


**Figure 5.** Simulated time traces (dots) for dye loaded zeolite L crystals with loadings  $p = 0.0028$ ,  $0.007$ , and  $0.014$ . Full lines are the exponential fit performed over each set of data. The simulations were performed on the molecular distributions estimated from CM images obtained in refs 33 and 57.

comparable to those of  $P_y^+$  and  $O_x^+$  which promote blocking of the channels as discussed above; longer guests on the other hand might reduce the wobbling motions in the channels,<sup>16,58</sup> thus favoring the diffusion process needed for the formation of fully loaded crystals.

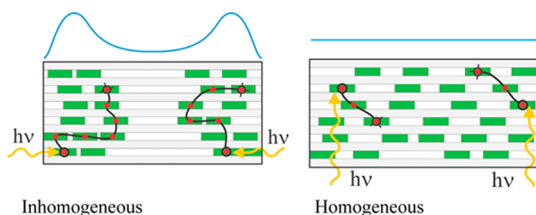


**Figure 6.** Illustration of the distribution of guest (green bars) in a homogeneous (right) and inhomogeneous way (left) inside a zeolite L crystal for high crystal loadings. Their impact in the RET dynamics is depicted by the different number of transfer steps (red circles) expected in a trajectory (indicated as black lines). The blue lines show the distribution of guests along the channels.

## 5. CONCLUSIONS

We have contributed to the understanding of the resonant energy transfer (RET) dynamics in dye-filled zeolite L host guest compounds (HGCs) through a computational approach relying on a quantum-chemical (QM) based diffusion-enhanced Förster-type RET, embedded in a macroscopic Monte Carlo (MC) scheme.

We have applied the QM/MC approach over the inhomogeneous distribution of the cationic dyes ( $P_y^+$  and  $O_x^+$ ) obtained from confocal microscopy images on  $P_y^+$  crystals, revealing that increasing inhomogeneity leads to a strong change in the exciton dynamics, reducing the exciton lifetimes and modifying the dimensionality of the transport.

The transient blocking regime may be avoided for instance by using longer guests, which would drastically reduce the wobbling motions inside the channels, favoring the molecular diffusion, thus favoring the homogeneous dye distributions. Such distribution together with the excellent RET transfer parameters of the pyronine/oxonine couple (large spectral overlaps, PL lifetime and exciton couplings), would deliver electronically efficient systems, with good stability, process-

ability, and addressability, that would make supramolecular nanostructured systems an even more interesting field of research in material science.

## AUTHOR INFORMATION

### Corresponding Authors

\*(L.V.) E-mail [lucas.viani@uc3m.es](mailto:lucas.viani@uc3m.es).

\*(J.G.) E-mail [johannes.gierschner@imdea.org](mailto:johannes.gierschner@imdea.org).

### ORCID

Hans-Joachim Egelhaaf: 0000-0002-4388-6556

Johannes Gierschner: 0000-0001-8177-7919

### Notes

The authors declare no competing financial interest.

## ACKNOWLEDGMENTS

L.V. is funded by the Universidad Carlos III de Madrid, the European Union's Seventh Framework Programme for research (grant agreement no. 600371), el Ministerio de Economía y Competitividad (COFUND2013-40258), and Banco Santander. The work at IMDEA has been supported by Ministerio de Economía y Competitividad, MINECO (CTQ2014-58801). The work in Mons is supported by the Interuniversity Attraction Pole program of the Belgian Federal Science Policy Office (PAI 7/05) and the Belgian National Fund for Scientific Research. D.B. and J.C. are FNRS Research Directors. This work was supported by the EC (grant no. MRTN-CT-2006-035884).

## REFERENCES

- Gierschner, J. Directional Exciton Transport in Supramolecular Nanostructured Assemblies. *Phys. Chem. Chem. Phys.* **2012**, *14*, 13146.
- Zabala Ruiz, A.; Li, H.; Calzaferri, G. Organizing Supramolecular Functional Dye-Zeolite Crystals. *Angew. Chem., Int. Ed.* **2006**, *45*, 5282–5287.
- Gierschner, J.; Lüer, L.; Oelkrug, D.; Musluoglu, E.; Behnisch, B.; Hanack, M. Preparation and Optical Properties of Oligophenylenevinylene/Perhydrotriphenylene Inclusion Compounds. *Adv. Mater.* **2000**, *12*, 757–761.
- Poulsen, L.; Jazdzzyk, M.; Communal, J.-E.; Sancho-García, J. C.; Mura, A.; Bongiovanni, G.; Beljonne, D.; Cornil, J.; Hanack, M.; Egelhaaf, H.-J.; et al. Three-Dimensional Energy Transport in Highly Luminescent Host-Guest Crystals: A Quantitative Experimental and Theoretical Study. *J. Am. Chem. Soc.* **2007**, *129*, 8585–8593.
- Botta, C.; Patrinoiu, G.; Picouet, P.; Yunus, S.; Cordella, F.; Communal, J.-E.; Quochi, F.; Mura, A.; Bongiovanni, G.; Pasini, M.; et al. Organic Nanostructured Host-Guest Materials Containing Three Dyes. *Adv. Mater.* **2004**, *16*, 1716–1721.
- Moreau, J.; Giovanella, U.; Bombenger, J.-P.; Porzio, W.; Vohra, V.; Spadacini, L.; Di Silvestro, G.; Barba, L.; Arrighetti, G.; Destri, S.; et al. Highly Emissive Nanostructured Thin Films of Organic Host-Guests for Energy Conversion. *ChemPhysChem* **2009**, *10*, 647–653.
- Srinivasan, G.; Villanueva-Garibay, J. A.; Müller, K.; Oelkrug, D.; Milian Medina, B.; Beljonne, D.; Cornil, J.; Wykes, M.; Viani, L.; Gierschner, J.; et al. Dynamics of Guest Molecules in PHTP Inclusion Compounds as Probed by Solid-State NMR and Fluorescence Spectroscopy. *Phys. Chem. Chem. Phys.* **2009**, *11*, 4996–5009.
- Viani, L.; Olivier, Y.; Athanasopoulos, S.; da Silva Filho, D. A.; Hulliger, J.; Brédas, J.-L.; Gierschner, J.; Cornil, J. Theoretical Characterization of Charge Transport in One-Dimensional Collinear Arrays of Organic Conjugated Molecules. *ChemPhysChem* **2010**, *11*, 1062–1068.
- Calzaferri, G.; Huber, S.; Maas, H.; Minkowski, C. Host-Guest Antenna Materials. *Angew. Chem., Int. Ed.* **2003**, *42*, 3732–3758.

- (10) Nguyen, T. Control of Energy Transfer in Oriented Conjugated Polymer-Mesoporous Silica Composites. *Science (Washington, DC, U. S.)* **2000**, *288*, 652–656.
- (11) Yatskou, M. M.; Meyer, M.; Huber, S.; Pfenniger, M.; Calzaferri, G. Electronic Excitation Energy Migration in a Photonic Dye–Zeolite Antenna. *ChemPhysChem* **2003**, *4*, 567–587.
- (12) Alohshyna, M.; Medina, B. M.; Poulsen, L.; Moreau, J.; Beljonne, D.; Cornil, J.; Di Silvestro, G.; Cerminara, M.; Meinardi, F.; Tubino, R.; et al. Oligophenylenevinylenes in Spatially Confined Nanochannels: Monitoring Intermolecular Interactions by UV/Vis and Raman Spectroscopy. *Adv. Funct. Mater.* **2008**, *18*, 915–921.
- (13) Gierschner, J.; Egelhaaf, H.-J.; Mack, H.-G.; Oelkrug, D.; Martínez Alvarez, R.; Hanack, M. Luminescence of Conjugated Molecules Confined in Nanochannels. *Synth. Met.* **2003**, *137*, 1449–1450.
- (14) Lupulescu, A. I.; Kumar, M.; Rimer, J. D. A Facile Strategy to Design Zeolite L Crystals with Tunable Morphology and Surface Architecture. *J. Am. Chem. Soc.* **2013**, *135*, 6608–6617.
- (15) Gigli, L.; Arletti, R.; Tabacchi, G.; Fois, E.; Vitillo, J. G.; Martra, G.; Agostini, G.; Quartieri, S.; Vezzalini, G. Close-Packed Dye Molecules in Zeolite Channels Self-Assemble into Supramolecular Nanoladders. *J. Phys. Chem. C* **2014**, *118*, 15732–15743.
- (16) Cao, P.; Khorev, O.; Devaux, A.; Sogger, L.; Kunzmann, A.; Ecker, A.; Häner, R.; Brühwiler, D.; Calzaferri, G.; Belser, P. Supramolecular Organization of Dye Molecules in Zeolite L Channels: Synthesis, Properties, and Composite Materials. *Chem. - Eur. J.* **2016**, *22*, 4046–4060.
- (17) Sancho-García, J. C.; Gierschner, J.; Poulsen, L.; Hennebicq, E.; Martínez-Alvárez, R.; Egelhaaf, H.-J.; Hanack, M.; Beljonne, D.; Oelkrug, D.; Cornil, J.; et al. Theoretical Characterization and Design of End-Substituted Distyrylbenzenes as Excitation Shuttles in One-Dimensional Channels. *Adv. Mater.* **2004**, *16*, 1193–1197.
- (18) Sancho-García, J. C.; Brédas, J.-L.; Beljonne, D.; Cornil, J.; Martínez-Alvarez, R.; Mart, R.; Hanack, M.; Poulsen, L.; Gierschner, J.; Mack, H.; et al. Design of Pi-Conjugated Organic Materials for One-Dimensional Energy Transport in Nanochannels. *J. Phys. Chem. B* **2005**, *109*, 4872–4880.
- (19) Hulliger, J.; Langley, P. J. Nanoporous and Mesoporous Organic Structures: New Openings for Materials Research. *Chem. Soc. Rev.* **1999**, *28*, 279–291.
- (20) Bongiovanni, G.; Botta, C.; Brédas, J.-L.; Cornil, J.; Ferro, D.; Mura, A.; Piaggi, A.; Tubino, R. Conformational Analysis and Optical Characterization of Oligothiophene Inclusion Compounds. *Chem. Phys. Lett.* **1997**, *278*, 146–153.
- (21) Komorowska, K.; Brasselet, S.; Dutier, G.; Ledoux, I.; Zyss, J.; Poulsen, L.; Jazdzzyk, M.; Gierschner, J.; Egelhaaf, H.-J.; Hanack, M. Nanometric Scale Investigation of the Nonlinear Efficiency of Perhydrotriphenylene Inclusion Compounds. *Chem. Phys.* **2005**, *318*, 12–20.
- (22) Couderc, G.; Hulliger, J. Channel Forming Organic Crystals: Guest Alignment and Properties. *Chem. Soc. Rev.* **2010**, *39*, 1545–1554.
- (23) Li, H.; Ding, Y.; Cao, P.; Liu, H.; Zheng, Y. Preparation and Luminescence of Transparent Zeolite L-Polymer Hybrid Materials. *J. Mater. Chem.* **2012**, *22*, 4056.
- (24) Devaux, A.; Calzaferri, G.; Belser, P.; Cao, P.; Brühwiler, D.; Kunzmann, A. Efficient and Robust Host–Guest Antenna Composite for Light Harvesting. *Chem. Mater.* **2014**, *26*, 6878–6885.
- (25) Gierschner, J.; Ehni, M.; Egelhaaf, H.-J.; Milián Medina, B.; Beljonne, D.; Benmansour, H.; Bazan, G. C. Solid-State Optical Properties of Linear Polyconjugated Molecules: Pi-Stack Contra Herringbone. *J. Chem. Phys.* **2005**, *123*, 144914.
- (26) Brühwiler, D.; Calzaferri, G.; Torres, T.; Ramm, J. H.; Gartmann, N.; Dieu, L.-Q.; López-Duarte, I.; Martínez-Díaz, M. V. Nanochannels for Supramolecular Organization of Luminescent Guests. *J. Mater. Chem.* **2009**, *19*, 8040.
- (27) Kehr, N. S.; El-Gindi, J.; Galla, H.-J.; De Cola, L. Click Chemistry on Self-Assembled Monolayer of Zeolite L Crystals by Microcontact Printing – Applications in Nanobiotechnology. *Microporous Mesoporous Mater.* **2011**, *144*, 9–14.
- (28) Wang, Y.; Li, H.; Feng, Y.; Zhang, H.; Calzaferri, G.; Ren, T. Orienting Zeolite L Microcrystals with a Functional Linker. *Angew. Chem., Int. Ed.* **2010**, *49*, 1434–1438.
- (29) Maas, H.; Calzaferri, G. Trapping Energy from and Injecting Energy into Dye-Zeolite Nanoantennae. *Angew. Chem., Int. Ed.* **2002**, *41*, 2284–2288.
- (30) Huber, S.; Calzaferri, G. Energy Transfer from Dye-Zeolite L Antenna Crystals to Bulk Silicon. *ChemPhysChem* **2004**, *5*, 239–242.
- (31) Calzaferri, G.; Méallet-Renault, R.; Brühwiler, D.; Pansu, R.; Dolamic, I.; Dienel, T.; Adler, P.; Li, H.; Kunzmann, A. Designing Dye-Nanochannel Antenna Hybrid Materials for Light Harvesting, Transport and Trapping. *ChemPhysChem* **2011**, *12*, 580–594.
- (32) Li, P.; Wang, Y.; Li, H.; Calzaferri, G. Luminescence Enhancement after Adding Stoppers to Europium(III) Nanozeolite L. *Angew. Chem., Int. Ed.* **2014**, *53*, 2904–2909.
- (33) Cucinotta, F.; Guenet, A.; Bizzarri, C.; Mróz, W.; Botta, C.; Milián-Medina, B.; Gierschner, J.; De Cola, L. Energy Transfer at the Zeolite L Boundaries: Towards Photo- and Electroresponsive Materials. *ChemPlusChem* **2014**, *79*, 45–57.
- (34) Dieu, L.-Q.; Devaux, A.; López-Duarte, I.; Martínez-Díaz, M. V.; Brühwiler, D.; Calzaferri, G.; Torres, T. Novel Phthalocyanine-Based Stopcock for Zeolite L. *Chem. Commun.* **2008**, No. 10, 1187–1189.
- (35) Chizhik, A. M.; Berger, R.; Chizhik, A. I.; Lyubimtsev, A.; Viani, L.; Cornil, J.; Bär, S.; Hanack, M.; Hulliger, J.; Meixner, A. J.; et al. Polarized Fluorescence from Single Stopcock Molecules at Channel Entrances of an All-Organic Host–Guest Compound. *Chem. Mater.* **2011**, *23*, 1088–1090.
- (36) Tsuiji, J.; Berger, R.; Labat, G.; Couderc, G.; Behrnd, N.-R.; Ottiger, P.; Cucinotta, F.; Schürmann, K.; Bertoni, M.; Viani, L.; et al. Alignment and Relaxation Dynamics of Dye Molecules in Host-Guest Inclusion Compounds As Probed by Dielectric Spectroscopy. *J. Phys. Chem. A* **2010**, *114*, 6956–6963.
- (37) Macchi, G.; Botta, C.; Calzaferri, G.; Catti, M.; Cornil, J.; Gierschner, J.; Meinardi, F.; Tubino, R. Weak Forces at Work in Dye-Loaded Zeolite Materials: Spectroscopic Investigation on Cation-Sulfur Interactions. *Phys. Chem. Chem. Phys.* **2010**, *12*, 2599–2605.
- (38) Fois, E.; Tabacchi, G.; Devaux, A.; Belser, P.; Brühwiler, D.; Calzaferri, G. Host-Guest Interactions and Orientation of Dyes in the One-Dimensional Channels of Zeolite L. *Langmuir* **2013**, *29*, 9188–9198.
- (39) Fois, E.; Tabacchi, G.; Calzaferri, G. Interactions, Behavior, And Stability of Fluorenone inside Zeolite Nanochannels. *J. Phys. Chem. C* **2010**, *114*, 10572–10579.
- (40) Gfeller, N.; Calzaferri, G. Energy Migration in Dye-Loaded Hexagonal Microporous Crystals. *J. Phys. Chem. B* **1997**, *101*, 1396–1408.
- (41) Viani, L.; Tolbod, L. P.; Jazdzzyk, M.; Patrinoiu, G.; Cordella, F.; Mura, A.; Bongiovanni, G.; Botta, C.; Beljonne, D.; Cornil, J.; et al. Spatial Control of 3D Energy Transfer in Supramolecular Nanostructured Host-Guest Architectures. *J. Phys. Chem. B* **2009**, *113*, 10566–10570.
- (42) Lencione, D.; Gehlen, M. H.; Trujillo, L. N.; Leitao, R. C. F.; Albuquerque, R. Q. The Spatial Distribution of the Photostability of Thionine in Zeolite L Nanochannels Investigated by Photobleaching Lifetime Imaging Microscopy. *Photochem. Photobiol. Sci.* **2016**, *15*, 398–404.
- (43) Calzaferri, G.; Lutkouskaya, K. Mimicking the Antenna System of Green Plants. *Photochem. Photobiol. Sci.* **2008**, *7*, 879–910.
- (44) Calzaferri, G. Nanochannels: Hosts for the Supramolecular Organization of Molecules and Complexes. *Langmuir* **2012**, *28*, 6216–6231.
- (45) Lutkouskaya, K.; Calzaferri, G. Transfer of Electronic Excitation Energy between Randomly Mixed Dye Molecules in the Channels of Zeolite L. *J. Phys. Chem. B* **2006**, *110*, 5633–5638.

- (46) Cucchi, I.; Spano, F.; Giovanella, U.; Catellani, M.; Varesano, A.; Calzaferri, G.; Botta, C. Fluorescent Electrospun Nanofibers Embedding Dye-Loaded Zeolite Crystals. *Small* **2007**, *3*, 305–309.
- (47) Vohra, V.; Calzaferri, G.; Destri, S.; Pasini, M.; Porzio, W.; Botta, C. Toward White Light Emission through Efficient Two-Step Energy Transfer in Hybrid Nanofibers. *ACS Nano* **2010**, *4*, 1409–1416.
- (48) Tsotsalas, M.; Busby, M.; Gianolio, E.; Aime, S.; De Cola, L. Functionalized Nanocontainers as Dual Magnetic and Optical Probes for Molecular Imaging Applications. *Chem. Mater.* **2008**, *20*, 5888–5893.
- (49) Tsotsalas, M. M.; Kopka, K.; Luppi, G.; Wagner, S.; Law, M. P.; Schäfers, M.; De Cola, L. Encapsulating  $^{111}\text{In}$  in Nanocontainers for Scintigraphic Imaging: Synthesis, Characterization, and in Vivo Biodistribution. *ACS Nano* **2010**, *4*, 342–348.
- (50) Gfeller, N.; Megelski, S.; Calzaferri, G. Fast Energy Migration in Pyronine-Loaded Zeolite L Microcrystals. *J. Phys. Chem. B* **1999**, *103*, 1250–1257.
- (51) Pfenniger, M.; Calzaferri, G. Intrazeolite Diffusion Kinetics of Dye Molecules in the Nanochannels of Zeolite L, Monitored by Energy Transfer. *ChemPhysChem* **2000**, *1*, 211–217.
- (52) Calzaferri, G.; Pauchard, M.; Maas, H.; Huber, S.; Khatyr, A.; Schaafsma, T.; Sciences, F. Photonic Antenna System for Light Harvesting, Transport and Trapping. *J. Mater. Chem.* **2002**, *12*, 1–13.
- (53) Megelski, S.; Lieb, A.; Pauchard, M.; Drechsler, A.; Glaus, S.; Debus, C.; Meixner, A. J.; Calzaferri, G. Orientation of Fluorescent Dyes in the Nano Channels of Zeolite L. *J. Phys. Chem. B* **2001**, *105*, 25–35.
- (54) Gasecka, A.; Dieu, L.-Q.; Brühwiler, D.; Brasselet, S. Probing Molecular Order in Zeolite L Inclusion Compounds Using Two-Photon Fluorescence Polarimetric Microscopy. *J. Phys. Chem. B* **2010**, *114*, 4192–4198.
- (55) Fois, E.; Tabacchi, G.; Calzaferri, G. Orientation and Order of Xanthene Dyes in the One-Dimensional Channels of Zeolite L: Bridging the Gap between Experimental Data and Molecular Behavior. *J. Phys. Chem. C* **2012**, *116*, 16784–16799.
- (56) Nakazato, S.; Takizawa, T.; Arai, T. Photoisomerization and Energy Transfer in Naphthalene-Terminated Stilbene Dendrimers. *Photochem. Photobiol. Sci.* **2012**, *11*, 885–888.
- (57) Busby, M.; Blum, C.; Tibben, M.; Fibikar, S.; Calzaferri, G.; Subramaniam, V.; De Cola, L. Time, Space, and Spectrally Resolved Studies on J-Aggregate Interactions in Zeolite L Nanochannels. *J. Am. Chem. Soc.* **2008**, *130*, 10970–10976.
- (58) Busby, M.; Devaux, A.; Blum, C.; Subramaniam, V.; Calzaferri, G.; De Cola, L. Interactions of Perylene Bisimide in the One-Dimensional Channels of Zeolite L. *J. Phys. Chem. C* **2011**, *115*, 5974–5988.
- (59) Zerner, M. C. Reviews in Computational Chemistry. In *Reviews in Computational Chemistry*; Lipkowitz, K. B., Boyd, D. B., Eds.; Wiley-VCH: New York, 1994; p 313.
- (60) Dewar, M. J. S.; Zoebisch, E. G.; Healy, E. F.; Stewart, J. J. P. Development and Use of Quantum Mechanical Molecular Models. 76. AM1: A New General Purpose Quantum Mechanical Molecular Model. *J. Am. Chem. Soc.* **1985**, *107*, 3902–3909.
- (61) The Structure Commission; [www.iza-structure.org](http://www.iza-structure.org), access date Jan 2016.
- (62) Tabacchi, G.; Calzaferri, G.; Fois, E. One-Dimensional Self-Assembly of Perylene-Diimide Dyes by Unidirectional Transit of Zeolite Channel Openings. *Chem. Commun.* **2016**, *52*, 11195–11198.